

Relating the physical structure and optical properties of conjugated polymers using neutron reflectivity in combination with photoluminescence spectroscopy

William J. Mitchell and Paul L. Burn^{a)}

The Dyson Perrins Laboratory, University of Oxford, South Parks Road, Oxford, OX1 3QY, United Kingdom

Robert K. Thomas

The Physical and Theoretical Chemistry Laboratory, University of Oxford, South Parks Road, Oxford, OX1 3QZ, United Kingdom

Giovanna Fragneto

Institut Laue-Langevin, 6, rue Jules Horowitz, B.P. 156, 38042 Grenoble Cedex 9, France

Jonathan P. J. Markham and Ifor D. W. Samuel

Organic Semiconductor Center, School of Physics & Astronomy, University of St Andrews, North Haugh, St Andrews, Fife, KY16 9SS, United Kingdom

(Received 21 July 2003; accepted 8 December 2003)

Understanding the effect of physical structure and the role of interfaces is critical for gaining insight into the optoelectronic properties of conjugated polymers and their behavior in semiconductor devices such as organic light-emitting diodes and photovoltaic cells. We have developed an *in situ* neutron reflection measurement that allows the direct relationship between film photoluminescence and structure to be studied. In addition, we have found that by judicious deuteration of the conjugated polymers, the polymer/indium tin oxide (ITO) interface can be probed. Critically for both poly[2-(2-*d*₁₇-ethylhexyloxy)-5-methoxy-1,4-phenylenevinylene] and poly[9,9'-(2-*d*₁₇-ethylhexyl)-2,6-fluorene] of thickness of order 140–150 nm on ITO, we found that a thermally stable low-density layer of 20 Å thickness was present between the polymer film and the ITO. The presence of the low-contact layer means that measurements involving these two families of polymers directly deposited onto ITO may need re-evaluating, and suggests why poly(3,4-ethylenedioxythiophene) poly(styrenesulfonate) may be so beneficial for polymer light-emitting diodes. © 2004 American Institute of Physics. [DOI: 10.1063/1.1644636]

I. INTRODUCTION

Conjugated polymers are being intensively investigated for a number of device applications, including organic light-emitting diodes (OLEDs), photovoltaics (PV), and field-effect transistors. Within these applications, it is clear that the morphology of the materials plays a critical role in controlling the properties of the polymers and the performance of the devices.^{1–7} In most of these studies, the morphology of the film has been inferred from the photophysical and device properties. However, there are few methods that can be used to probe the physical structure of polymer films at the same time as their emissive properties.⁸ Another critical aspect to consider is the interfaces between each of the layers in the device, including, perhaps most critically, the conjugated-polymer/electrode interface.^{9–11} For example, when poly(3,4-ethylenedioxythiophene) poly(styrenesulfonate) (PEDOT) was used as a layer between an indium tin oxide (ITO) anode and the light-emitting polymer in an OLED, a dramatic improvement in device lifetime was observed. Although there are many techniques for studying exposed surfaces of films, there are fewer techniques for studying buried interfaces. We have used neutron reflection (NR) as a pow-

erful technique for the study of the effect of different processing conditions on conjugated-polymer morphology.^{12,13} Although most NR studies on polymer films have so far been carried out on silicon substrates, and hence do not reveal the effect of polymer/electrode interactions, we have reported recently that it is possible to carry out NR studies of polymer films directly on ITO, a commonly used anode for OLEDs and PV cells.¹³

In this article, we report NR studies on examples of the two most widely studied and commercially significant families of soluble conjugated polymers: polymers based on poly(1,4-phenylenevinylene) and poly(2,6-fluorene) on ITO. The materials studied were poly[2-(2-*d*₁₇-ethylhexyloxy)-5-methoxy-1,4-phenylenevinylene] (MEHPPV) and poly[9,9'-(2-*d*₁₇-ethylhexyl)-2,6-fluorene] (PF). We illustrate how combined photoluminescence (PL) and NR can be used to gain a fundamental understanding of the relationship between polymer morphology and emissive properties, and demonstrate how the use of partially deuterated polymers can give valuable information about the polymer/ITO interface.

II. EXPERIMENT

The ITO used in this investigation was from Merck Display Technologies (Part No: 255 645 XE, 20 Ω/square) and

^{a)}Electronic mail: paul.burn@chem.ox.ac.uk

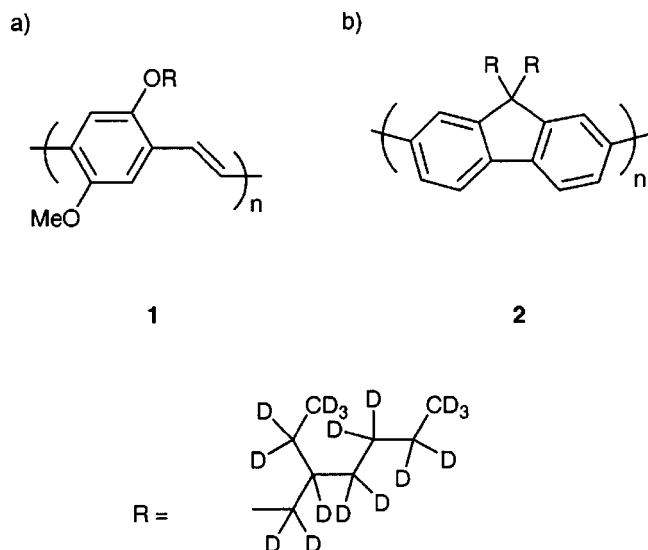


FIG. 1. Polymer structures: (a) MEHPPV and (b) PF.

consisted of (in order) soda lime glass, a silicon dioxide barrier layer, and a 100 nm layer of ITO. The MEHPPV (**1**) and PF (**2**) both had perdeuterated 2-ethylhexyl groups (Fig. 1). \bar{M}_w and polydispersity (p.d.) of **1** and **2** used in this study were determined by gel-permeation chromatography (against polystyrene standards in tetrahydrofuran). For **1**, $\bar{M}_w = 1.5 \times 10^6$ and p.d. = 21, and for **2**, $\bar{M}_w = 1.2 \times 10^6$ and p.d. = 11. Before spin-coating, the ITO substrates were cleaned by washing with tetrahydrofuran. For the NR experiments, **1** was spin-coated onto 50 mm² ITO substrates with a polymer concentration ≈ 7 mg/mL in tetrahydrofuran at 2000 rpm for 60 s. **2** was spin-coated under the same conditions, but at a concentration ≈ 10 mg/mL. The glass transition temperatures of **1** and **2** were measured by differential scanning calorimetry under helium and were found to be 196 °C (scan rate = 200 °C/min) and 93 °C (scan rate = 100 °C/min), respectively. NR profiles were collected for **1** and **2** at various temperatures, including above the glass transition temperatures. A NR profile is a measure of the specular reflectivity as a function of the wave-vector transfer perpendicular to the interface, q [$q = (4\pi \sin \theta)/\lambda$, where θ is the angle between the neutron beam and the plane of the substrate and λ is the wavelength of the neutron]. NR measurements were carried out under a dynamic vacuum on the dedicated reflectometer D17,¹⁴ at the Institut Laue-Langevin, Grenoble, in the time-of-flight mode with a wavelength range of 0.2 to 2 nm, at an angle $\theta = 0.7^\circ$ and resolution $\Delta q/q = 1\%$. The *in situ* PL measurements were carried out simultaneously using a 408 nm nitride laser for excitation and a fiber-coupled Ocean Optics CCD spectrograph for detection.

III. RESULTS AND DISCUSSION

To determine the physical structures of the polymers on the ITO, it was first necessary to characterize the ITO by NR. The NR profile can be determined by the profile of the scattering length density ρ across the interface, which depends on the number density of each atomic species n_i and its known scattering length b_i .¹⁵

$$\rho = \sum_i n_i b_i.$$

When the stoichiometry and isotopic composition are known, as with the polymers in this work, this equation can be rewritten in terms of the segment density ρ_s of the polymer film:

$$\rho = b_s \rho_s,$$

where b_s is the scattering length of a monomer unit. In the simplest case of a uniform film of polymer, the NR profile consists of a series of fringes whose spacing is directly related to the thickness of the film. The segment density of the film can be determined either from the amplitude of the fringes or, if the scattering length density of the film is greater than that of the substrate and the film thickness is greater than about 40 nm, from the critical angle for total reflection. The latter criterion was met when partially deuterated polymers were deposited on silicon substrates.¹² The ability to identify the scattering length density from the critical angle of reflection is helpful because the reflectivity profile can be complicated by factors such as roughness in such a way that the amplitude of the fringes is not easily related to the film density. As the roughness of a film increases, the interference fringes become progressively more damped and, under these circumstances, the behavior of the amplitude of the fringes gives more information about the roughness than about the density of the film. For more complex film structures, as in this study, the reflectivity is fitted by comparison of the observed reflectivity, with profiles calculated using the optical matrix method, for which a detailed description has been given by Born and Wolf¹⁶ and Lekner.¹⁷ In the optical matrix method, the reflectivity can be calculated exactly for any chosen distribution of scattering length density normal to the interface. The procedure that we have followed uses the minimum number of subdivisions of the film structure required to obtain the best fit to the data. The two key parameters that can be extracted from the NR data are the thicknesses and scattering length densities (SLDs) of the component layers; in addition, some qualitative information about the nature of their roughness can be gained. The errors in the determined thicknesses and SLDs, except where it is stated otherwise, have been assessed as the range over which the fits, shown in the figures, are acceptable.

In the case of ITO on glass, the film is approximately uniform, and hence the NR profile consists of a series of fringes whose spacing is directly related to the thickness of the film. The NR profile and fit for the ITO on glass substrates are shown in Fig. 2. Using the optical matrix method, the ITO layer was determined to consist of an 8 ± 2 nm thick component with a SLD of $5.0 \pm 0.1 \times 10^{-6} \text{ \AA}^{-2}$ next to the glass, with the remainder of the ITO film being 112 ± 2 nm thick with a SLD of $4.0 \pm 0.1 \times 10^{-6} \text{ \AA}^{-2}$. The rms roughness of the composite layer was determined to be approximately 3.5 nm.¹³ The rms roughness of the composite film determined from the NR profile compares well to the 2.7 nm rms surface roughness of the film measured by atomic force microscopy (AFM).

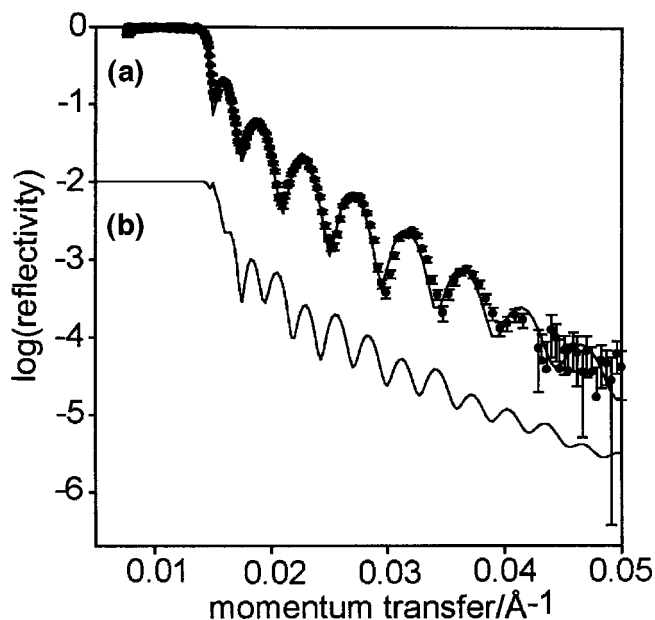


FIG. 2. (a) Measured NR profile and fit (solid line) of ITO on glass and (b) calculated NR profile for a polymer film deposited on ITO on glass, where the polymer film and ITO have similar scattering length densities (see Ref. 13).

The fact that the SLD of the ITO and the partially deuterated polymers are similar has enabled us to probe the interface between the ITO and polymer layers. When two layers have similar SLDs, the NR profile in going from a single

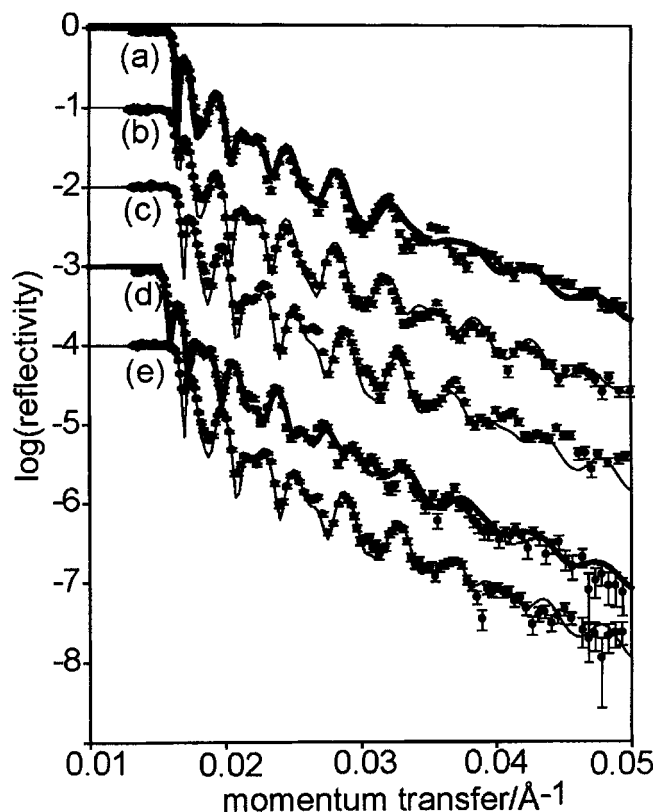


FIG. 4. Measured NR profiles and fits (solid lines) of PF at (a) RT; (b) 120 °C; (c) RT after 120 °C anneal; (d) 220 °C; and (e) RT after 220 °C anneal. The reflectivity scale corresponds to the profile for (a). The other plots are offset successively by subtraction of 1 for clarity.

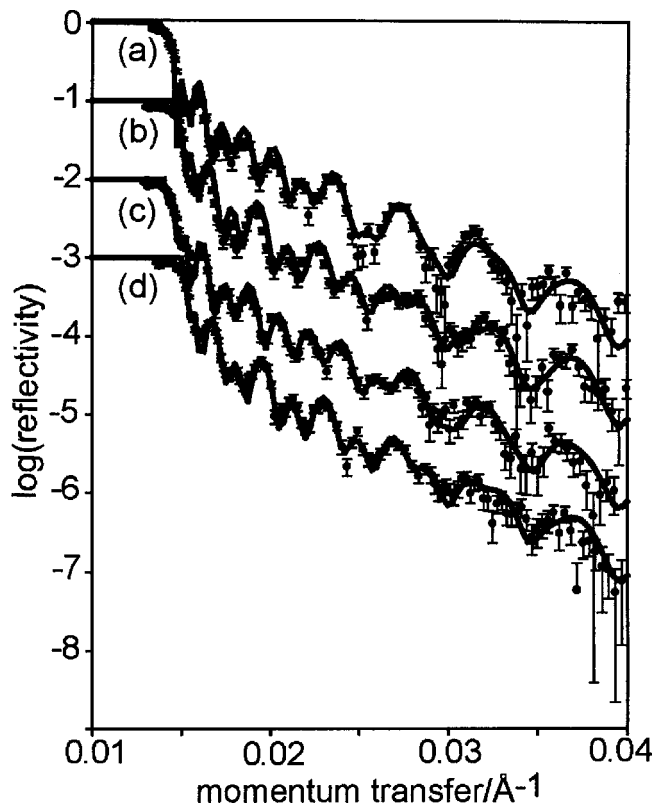


FIG. 3. Measured NR profiles and fits (solid lines) of MEHPPV at (a) RT; (b) 70 °C; (c) 220 °C; (d) RT (34° C) after 220 °C anneal. The reflectivity scale corresponds to the profile for (a). The other plots are offset successively by subtraction of 1 for clarity.

layer of one material to a bilayer of the two materials should simply be a profile corresponding to the thicker film. That is, the periodicity of the fringes should simply increase for the overall thicker film, and there should be no differentiation between the two layers. This is illustrated by the calculated profile in Fig. 2(b). As can be seen in Figs. 3 and 4, the deposition of the polymer layer has not simply caused an increase in the periodicity of the fringes, but has given rise to a much more complicated reflection profile. As discussed in a previous paper, the presence of a depleted, or low-contact, region is revealed by the strong effect of such a layer on the interference pattern when separating two layers of comparable scattering length density.¹³ The thickness of the low-contact layer (LCL) is comparable to the interlayer rms roughness used to fit the data, here approximately 3.5 nm. As a consequence, the LCL can be fitted with a range of parameters for thickness and scattering length density. However, the important model-independent result is that there is a definite amount of polymer missing from the interfacial region, although how it is distributed is less certain. For example, it could vary from almost no polymer (zero scattering length density) and thickness t , to 50% polymer and thickness $2t$. The LCL could be caused by a number of reasons, including the failure of the polymer to wet the ITO surface, ITO asperities supporting the fairly rigid, thick layer of polymer, or the loss of an intervening layer of spreading solvent on evaporation under vacuum.

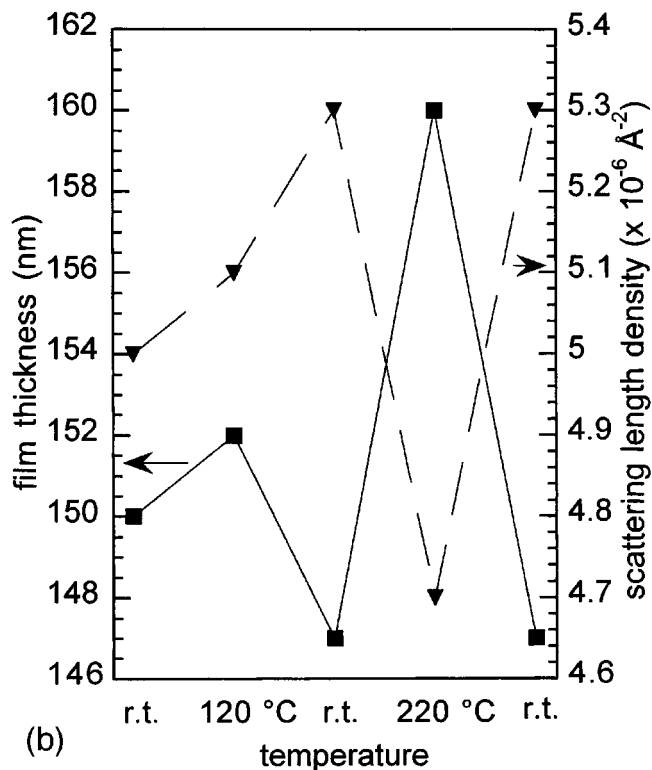
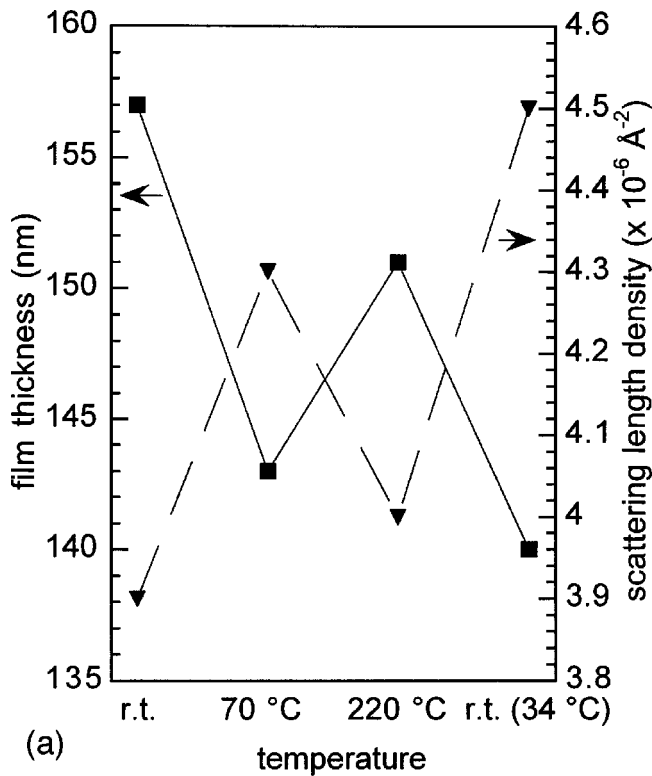


FIG. 5. Summaries of the scattering length density (triangles) and film thickness (squares) determined from the NR profiles versus temperature: (a) MEHPPV and (b) PF.

A. MEHPPV

We next consider the results for MEHPPV in more detail. Figure 3 shows the reflectivity profiles of MEHPPV at various points during a thermal cycle in which the sample is heated to 220 °C and then allowed to cool back to room

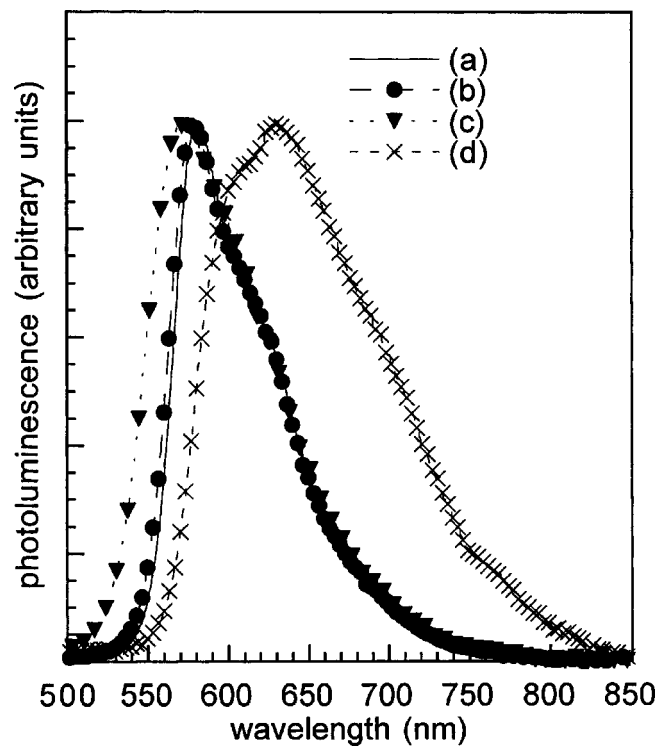


FIG. 6. PL spectra of MEHPPV at (a) RT; (b) 70 °C; (c) 220 °C; and (d) RT after 220 °C anneal.

temperature (RT). The results are shown for RT (before heating), 70 °C, 220 °C, and RT (after heating), and a summary of the polymer film thicknesses and scattering length densities is shown in Fig. 5(a). At each temperature, the NR profile and PL spectrum were acquired, and the PL spectra shown in Fig. 6. The reflectivity profile and fit for the as-spun

MEHPPV are shown in Fig. 3(a). From the reflectivity profile, the thickness of the polymer film was determined to be 157 ± 2 nm and it had a SLD of $3.9 \pm 0.1 \times 10^{-6} \text{ \AA}^{-2}$. For all measurements, the LCL could be fitted reasonably within the limits of thickness of 1.5–4.0 nm, with the layer being comprised of 100% to 40% empty space. A SLD of around zero corresponds to 100% empty space and, although the NR profile can be fitted with the LCL having a SLD of zero, there must still be contact points to the ITO as the polymer was firmly adhered to the substrate. The best fit for the intermediary LCL, which is stable to the thermal cycling, between the polymer and the ITO, was for the layer to be 1.5 nm thick with a negligible SLD. Poor contact between the polymer layer and the electrode will lead to poor charge injection and, if the layer contains air, can lead to oxidative degradation. Therefore, this result has important implications for devices prepared by depositing the polymer directly onto the electrode surface.

When the film was heated to 70 °C, there was a marked decrease in the film thickness and an increase in the SLD. The film thickness reduced by 9% to 143 ± 2 nm and the SLD increased by around 10% to $4.3 \pm 0.1 \times 10^{-6} \text{ \AA}^{-2}$. Such a change could be due to either the removal of solvent or the rearrangement of the polymer in the film. We believe that the change in the film thickness and density is due to the

latter and not to the removal of solvent, as the change would require the film to be made up of around 10% of solvent. Such a high level of solvent in the film is highly unlikely, as the measurements are carried out under dynamic vacuum. Given that 70 °C is well below the T_g (196 °C) of this sample of MEHPPV in the polymer bulk, the densification most probably arises from the rearrangement of the polymer chains enabled by the bulky, flexible 2-ethylhexyloxy side groups. Heating the film to 220 °C, which is above the T_g of MEHPPV, the film expanded, with the thickness increasing by 8 nm (6%) to 151 ± 2 nm and the SLD decreasing by the commensurate amount to $4.0 \pm 0.1 \times 10^{-6} \text{ \AA}^{-2}$ (7%). Finally, after cooling to near RT, the final profile was measured. The final thickness and SLD of the MEHPPV film were $4.5 \pm 0.1 \times 10^{-6} \text{ \AA}^{-2}$ and 140 ± 2 nm, respectively. Therefore, after thermal annealing, the total film thickness decreased by 17 nm and the density increased by 15%. The fact that MEHPPV anneals significantly at 70 °C is important for device manufacturing and testing, as it is well within the temperature range at which devices might be prepared and used.

Taking the results from the NR profiles on their own, it is not possible to determine whether the polymer is completely annealed at 70 °C or whether there is a second annealing process at the higher temperature that could correspond to the reordering of the conjugated polymer backbone. However, by combining the PL measurements (Fig. 6), it is possible to elucidate what is happening in the film. At RT, the typical MEHPPV film spectrum is observed with a peak at 581 nm and a shoulder at 625 nm. At 70 °C, there is only a small change in the PL spectrum in spite of the large decrease in film thickness and increase in SLD. This initially suggests that an increase in film density by more efficient packing of the polymer chains can occur without an increase in π - π interactions that cause excimer emission. However, it is important to remember that MEHPPV films expand on heating.¹² Therefore, although the film has contracted at 70 °C, it might still be expanded relative to what it would be at RT. This element of thermal expansion could be enough to reduce π - π stacking and to avoid additional excimer emission. On going from 70 to 220 °C, the long-wavelength side of the PL emission is the same as at lower temperatures, but the peak and blue edge of the spectrum has moved to shorter wavelengths. This is consistent with more disorder in the conjugated backbone associated with the expanded film. On cooling to RT after the high-temperature anneal, there was a large redshift in the emission peak and increased red tail, both of which are normally associated with better intramolecular order and increased π - π interactions.⁵ However, the question still remains as to whether densification of the film at 70 °C also leads to excimer emission in a cooled film. To resolve this, we measured the PL of a sample at RT after it had been annealed at 70 °C. There was only a small redshift, on the order of a few nanometers, in the PL spectrum, and not the large redshift and long red tail indicative of excimer emission in MEHPPV. This, in conjunction with the NR results, indicates that MEHPPV can pack effectively at a temperature well below its T_g , with only a small effect on the emissive properties. However, the device properties of an

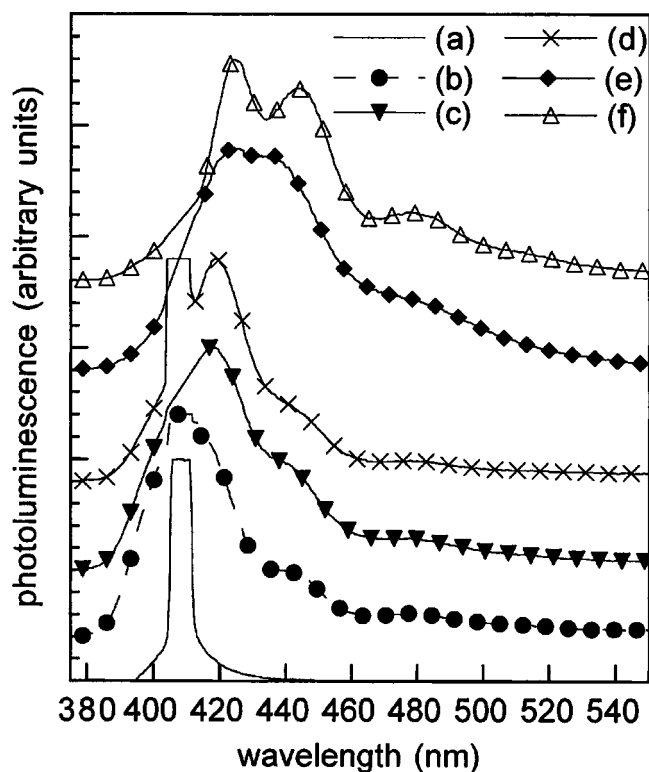


FIG. 7. PL spectra of (a) the laser emission and PF at (b) RT; (c) 120 °C; (d) RT after 120 °C anneal; (e) 220 °C; and (f) RT after 220 °C anneal. The spectra are offset for clarity.

MEHPPV film after a low-temperature anneal may well be different from an as-deposited film.

B. PF

The rigid-rod PF used in this study has been reported to be a nematic liquid crystal, and hence the PF and MEHPPV films were expected to behave differently.¹⁸ For the PF film, we measured the NR profiles at RT, then 120 °C, RT, 220 °C, and then RT again. The corresponding NR profiles of the PF film are shown in Fig. 4 and are summarized Fig. 5(b). The key result from Fig. 4 was the observation of the presence of a LCL between the PF film and the ITO. As in the case of MEHPPV, the LCL was present under all thermal conditions, could be fitted reasonably with a thickness range of 3–5 nm, and was comprised of 100% to 60% empty space. At RT, the as-deposited polymer layer was found to be 150 ± 2 nm thick with a SLD of $5.0 \pm 0.1 \times 10^{-6} \text{ \AA}^{-2}$. On heating the film to 120 °C, which is above the T_g of **2** in the bulk, there was only a small change in thickness and, on cooling back to RT, the film thickness was found to decrease by only 3 nm or 2% when compared with the initial RT measurement. There was a concomitant increase in the SLD to $5.3 \pm 0.1 \times 10^{-6} \text{ \AA}^{-2}$ (6%) showing a densification of the film; that is, the film had annealed slightly. At 220 °C, the PF film thermally expanded to 160 ± 2 nm and it had a SLD of $4.7 \pm 0.1 \times 10^{-6} \text{ \AA}^{-2}$. On cooling to RT, the PF film thickness and SLD returned to those observed after the first thermal cycle to 120 °C, suggesting that the annealing of the PF film occurred after the first heating. The smaller changes in film thickness and SLD on annealing of the PF film when compared to the MEHPPV

film is consistent with it being a more rigid polymer, and indicates that the as-deposited film is better ordered.

The PL spectra of the PF taken at the different temperatures are shown in Fig. 7. The short-wavelength peaks are complicated due to the presence of a spike caused by the excitation wavelength (408 nm) and the excitation geometry used. Nevertheless, the trends in the spectra at longer wavelengths are clear. At RT, the as-deposited film has the typical PF spectrum, with a shoulder at 475 nm corresponding to emission from aggregates. On heating to 120 °C, which is above the T_g (93 °C) of the PF, and then cooling to RT, there is only a small redshift in the PL spectrum in spite of the small increase in density. On heating the polymer to 220 °C, the NR profile showed that the film had expanded. The PL spectrum at 220 °C was broader than at the lower temperature, and there was no significant blueshift at the short-wavelength edge of the emission spectrum. In addition, the PL spectrum showed an increase in the long-wavelength emission when compared with the as-deposited film. This behavior is in contrast to MEHPPV and is due to the more rigid-rod nature of the PF. On cooling back to RT, although the NR profile shows that the film thickness and density have not changed when compared to the thermal anneal at 120 °C, the PL spectrum shows that the film is more ordered, with a small redshift in the emission maximum, well-defined vibronic structure, and increased proportion of aggregate emission. The increase in order shown in the PL spectrum is consistent with it going into the nematic phase, but it is interesting that there is no associated increase in film density.

IV. CONCLUSION

We have shown that combining PL spectroscopy and NR gives rise to a powerful technique for relating the physical structure to the optical properties of conjugated polymers. In addition, the combination of partially deuterated polymers deposited on ITO has allowed the probing of the polymer/electrode interface. Crucially, we have found that the simple deposition of 140–150 nm thick films of MEHPPV and PF from tetrahydrofuran onto ITO can give rise to stable low

contact layers (LCLs) between the ITO and polymer layer. The LCL will effect charge injection from the electrode to the polymer layer, leading to poor device performance, and the presence of air in the low-contact region could also lead to accelerated device degradation. The presence of this LCL may explain why hole injection layers such as PEDOT give improved LED lifetime and performance.

ACKNOWLEDGMENTS

We thank Sharp Laboratories of Europe Ltd for Awards (W. J. M. and J. P. J. M.), and measuring the rms roughness of the ITO by AFM. One of the authors (I. D. W. S.) is a Royal Society University Research Fellow.

- ¹T-Q. Nguyen, R. C. Kwong, M. E. Thompson, and B. J. Schwartz, *Appl. Phys. Lett.* **76**, 2454 (2000).
- ²T-Q. Nguyen, V. Doan, and B. J. Schwartz, *J. Chem. Phys.* **110**, 4068 (1999).
- ³J. Liu, Y. Shi, L. Ma, and Y. Yang, *J. Appl. Phys.* **88**, 605 (2000).
- ⁴Y. Shi, J. Liu, and Y. Yang, *J. Appl. Phys.* **87**, 4254 (2000).
- ⁵T-Q. Nguyen, I. B. Martini, J. Liu, and B. J. Schwartz, *J. Phys. Chem. B* **104**, 237 (2000).
- ⁶A. K. Sheridan, J. M. Lupton, I. D. W. Samuel, and D. D. C. Bradley, *Chem. Phys. Lett.* **322**, 51 (2000).
- ⁷J. Liu, Y. Shi, and Y. Yang, *Adv. Funct. Mater.* **11**, 420 (2001).
- ⁸T.-F. Guo and Y. Yang, *Appl. Phys. Lett.* **80**, 148 (2002).
- ⁹P. K. H. Ho, J.-S. Kim, J. H. Burroughes, H. Becker, S. F. Y. Li, T. M. Brown, F. Cacialli, and R. H. Friend, *Nature (London)* **404**, 481 (2000).
- ¹⁰S.-C. Lo, L.-O. Pålsson, M. Kilitziraki, P. L. Burn, and I. D. W. Samuel, *J. Mater. Chem.* **11**, 2228 (2001).
- ¹¹V. Bliznyuk, B. Ruhstaller, P. J. Brock, U. Scherf, and S. A. Carter, *Adv. Mater. (Weinheim, Ger.)* **11**, 1257 (1999).
- ¹²G. R. Webster, W. J. Mitchell, P. L. Burn, R. K. Thomas, G. Fragneto, J. P. J. Markham, and I. D. W. Samuel, *J. Appl. Phys.* **91**, 9066 (2002).
- ¹³W. J. Mitchell, P. L. Burn, R. K. Thomas, and G. Fragneto, *Appl. Phys. Lett.* **82**, 2724 (2003).
- ¹⁴R. Cubitt and G. Fragneto, *Appl. Phys. A: Mater. Sci. Process.* **74**[Suppl.], S329 (2002).
- ¹⁵R. K. Thomas, in *Scattering Methods in Polymer Science*, edited by R. W. Richards (Ellis Horwood, London, 1995).
- ¹⁶M. Born and E. Wolf, *Principles of Optics*, 6th ed. (Pergamon, Oxford, 1980).
- ¹⁷J. Lechner, *Theory of Reflection* (Martinus Nijhoff, Dordrecht, 1987).
- ¹⁸M. Grell, W. Knoll, D. Lupo, A. Meisel, T. Miteva, D. Neher, H.-G. Nothofer, U. Scherf, and A. Yasuda, *Adv. Mater. (Weinheim, Ger.)* **11**, 671 (1999).